JACS
JOURNAL OF THE AMERICAN CHEMICAL SOCIETY

ARTICLE

pubs.acs.org/JACS

Controlling the Position of Functional Groups at the Liquid/Solid Interface: Impact of Molecular Symmetry and Chirality

Inge De Cat,[†] Cristian Gobbo,[‡] Bernard Van Averbeke,[§] Roberto Lazzaroni,[§] Steven De Feyter,*[,†] and Jan van Esch*[,‡]

[†]Department of Chemistry, Division of Molecular Imaging and Photonics, Katholieke Universiteit Leuven, Celestijnenlaan 200F, 3001 Leuven, Belgium

[‡]Department of Chemistry, Laboratory of Self-assembling Systems, Delft University of Technology, Julianalaan 136, 2628 BL Delft, The Netherlands

[§]Laboratory for Chemistry of Novel Materials, Université de Mons, Place du Parc 20, 7000 Mons, Belgium

Supporting Information

ABSTRACT: With the aim of controlling the position of functional groups in a substrate-supported monolayer, a new family of functionalized linear alkyl chains was designed and synthesized, aided by molecular mechanics and dynamics simulations of its two-dimensional self-assembly on graphite. The self-assembly of these amino functionalized diamides at the liquid/solid interface was investigated with scanning tunneling microscopy. Intermolecular hydrogen-bonding interactions involving amides, combined with the effect of molecular symmetry and chirality, were found to guide the self-assembly. Control of the relative position and orientation of the amine groups was achieved, in the case of enantiopure compounds. Interestingly, racemates led to both racemic conglomerate and solid solution formation, with a concomitant loss of positional and orientational control of the amino groups as a result.

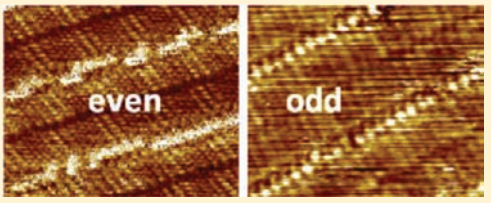

INTRODUCTION

Due to the continuing need for miniaturization of functional interfaces, the bottom-up patterning of interfaces by molecular self-assembly is receiving growing attention as an alternative for top-down nanopatterning techniques.[1−9] Self-assembled monolayers (SAMs), and in particular the alkyl thiols−gold-based systems have extensively been used to tune the interfacial properties via, e.g. the exposure of specific chemical functions,[10,11] for applications such as (bio)molecular recognition,[12−15] heterogeneous catalysis,[16−19] and sensor technology.[20,21] Many of these applications will benefit from the in-plane ordering of chemical function. However, despite few examples,[22−24] chemisorbed SAMs displayed little control over the formation of well-defined patterns at 1−20-nm length scales with subnanometer resolution by bottom-up assembly only.[25−28]

In contrast to chemisorbed SAMs, physisorbed molecular monolayers have extensively been exploited to create a wide variety of molecular patterns with lattice constants of typically 1−20 nm.[29−33] For instance, on highly oriented pyrolytic graphite (HOPG), long alkanes and their derivatives self-assemble into a regular lamellar lattice parallel to the surface.[34−39] High-quality pattern formation in such physisorbed monolayers is facilitated by their dynamic nature, owing to the stabilization of the molecular monolayers by only noncovalent interactions.[40−49] Recently, it was shown that the pattern of such physisorbed monolayers could be stabilized by postpolymerization.[50−54] Most remarkably, in spite of their flexibility in pattern formation and their broad use as model systems to study two-dimensional (2D) molecular self-assembly, physisorbed SAMs are still waiting to be exploited as a platform for the defined spatial deposition of chemical functions at liquid/solid interfaces.

It is the aim of this contribution to utilize physisorbed SAMs for the defined deposition of functional elements at the liquid/solid interface, and to investigate the impact of molecular symmetry and chirality on the 2D arrangement of these functional elements. Therefore, a new family of chiral amino-functionalized diamides (ADA) was designed (Figure 1) aided by molecular modeling and dynamics simulations, and the self-assembly of these molecules was studied with scanning tunneling microscopy (STM) at the liquid/solid interface. The long alkyl chains are likely to self-assemble parallel to the substrate due to their commensurability with the graphite surface.[34] This will force the amine functionality to be oriented away from the plane. By varying the number of methylene groups (n) between the amides, the relative orientation of the interacting units will be parallel or opposite. In addition, the absolute configuration of the stereogenic center and the composition of the solute, i.e. containing an enantiopure compound versus a racemate can be changed. These factors allow us to control the pattern formation, including the position and orientation of the amino groups. Key insights were also obtained on the role of stereogenic centers in the self-assembly process.

Received: September 25, 2011
Published: December 01, 2011

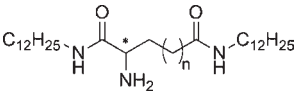

Figure 1. Chiral amino-functionalized diamides (X-ADAm). $m = n + 2$ is the number of methylene groups between the two amides and X (*R* or *S*) is the absolute configuration. The asterisk represents a stereogenic center.

RESULTS AND DISCUSSION

Design. To exploit the potential of physisorbed SAMs for the spatially controlled positioning of functional groups at interfaces, amino functionalized diamides (ADA) have been chosen as a model molecular platform. The choice of alkyl diamides is inspired by the positive experience with alkyl bis-urea compounds, which are known to form lamellar molecular arrays on HOPG, directed by the hydrogen-bonding interactions between the urea moieties.[38] An amine moiety was chosen as a generic functionality because it can be differentiated from alkyl chains by scanning tunneling microscopy (STM)[41] and, at later stages, can act as a versatile center of reactivity for further functionalization.

The design of simple amino functionalized diamides is complicated by the fact that the addition of even a single amine function to an alkyl chain (1) leads to the creation of a stereogenic center and (2) leads to desymmetrization of the alkyl diamide scaffold (unless the amine function is positioned in a mirror plane). As a consequence, several packing modes are possible which may lead to polymorphism and/or positional disorder of the functional groups (Figure 2a). When considering the relative stabilities of the possible arrangements, a configuration where the functionality points down toward the substrate is likely to be less stable for steric reasons then a configuration where the amine group points upward. Furthermore, formation of 1D hydrogen-bonded arrays is also likely to increase the stability.

Under these assumptions, a first analysis showed that the role of several structural elements needs to be considered for the design of functionalized bisamide scaffolds (Figure 2). (i) Stereogenic centers; the presence of stereogenic centers may offer possibilities to control the relative orientation of the functional groups (Figure 2a,b), but also may lead to additional disorder and polymorphism if racemic compounds are being used (Figure 2a). (ii) Hydrogen bonding and parity of the methylene groups; in the case of antiparallel oriented amides, 2-fold rotation around an axis perpendicular to the surface would preserve hydrogen-bonding interactions with neighboring molecules within one lamella, but would result in positional disorder of functional groups without such a symmetry element within the same molecule (Figure 2c). Also for parallel oriented hydrogen-bonding groups, positional disordering of chemical functional moieties while preserving the hydrogen-bonded arrays would arise from 2-fold rotation around an axis parallel to the lamellar axis (Figure 2d). In the case of alkyl spacers between the amides, the relative orientation of the amides depends on the parity of the methylene groups within the spacer.[55−59]

From this analysis it is clear that incorporation of a simple functionality like an amine moiety into the alkyl bis-amide scaffold may potentially lead to several polymorphic packing modes, with or without positional disorder of the amine functionalities. Moreover, the effect of the structural elements discussed above on the packing mode depends on the presence of the other elements.

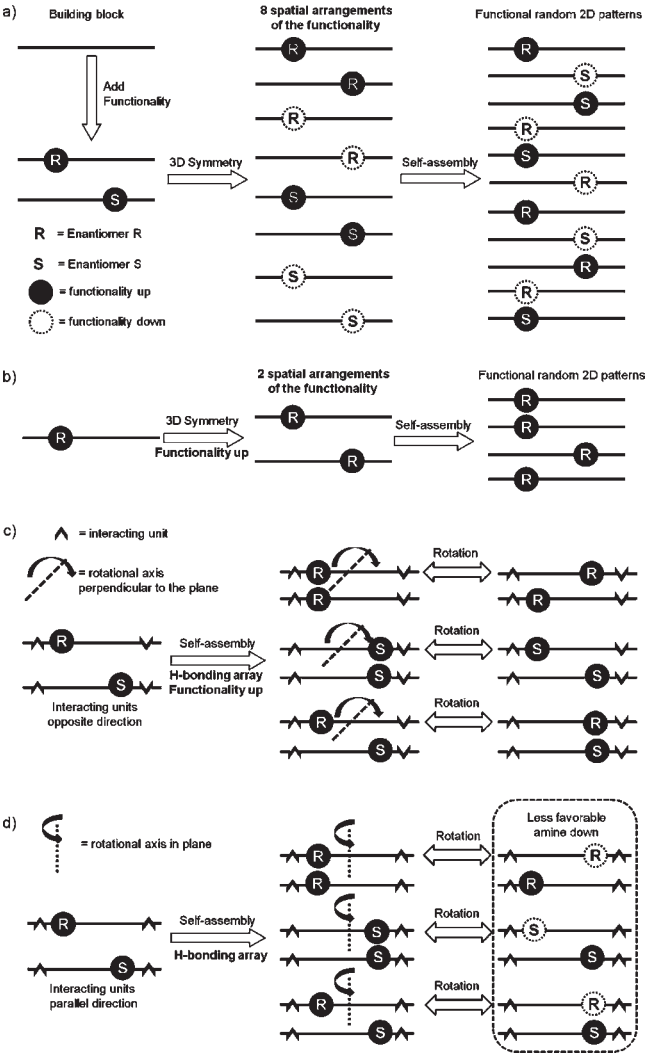

Figure 2. Design principle. (a) Replacing a hydrogen atom from a linear alkyl building block with a functional group generates two enantiomers (racemate), assuming that no meso-compound can be formed. In principle, these enantiomers can form, in total, eight spatial arrangements in a plane. Those with the functionality down, thus facing a surface, are considered to be less stable. Lack of a distinct difference in stability between homochiral and heterochiral interactions will lead to disordered patterns. (b) Enantiopure molecules reduce the possible spatial arrangements. In the absence of intermolecular interactions affecting the relative orientation of adjacent molecules, these supramolecular tapes will still show a high degree of disorder. (c, d) Introducing two directional units within the same molecule, which point in antiparallel (c) or parallel (d) directions, is key for controlled self-assembly. In the antiparallel case (c), only rotation of a molecule over 180° along an axis perpendicular to the surface plane preserves the directional intermolecular interactions, though with a loss of positional control of the functional groups as result. In the parallel case (d), for similar reasons, only rotation over 180° along an axis parallel to the tape axis preserves the directional intermolecular interactions, but 'functionality up' becomes 'functionality down', which is unfavorable. In absence of this rotation, positional control is potentially achieved.

In Tables 1 and 2 several different possible packing modes are depicted for simple enantiomerically pure ADA molecules with parallel or antiparallel oriented amide groups. It should be noted that the possible packings are likely to have different stability.

Table 1. Possible Packing Arrangements for an Enantiopure Odd Molecule (illustrated for R-ADA5) with Their Total Potential Energy, Valence and Nonbond Energy per Mole Molecule [a]

Packing	Model	Total potential Energy (kcal/mol)	Valence Energy / Non-bond Energy
1-AupRCs	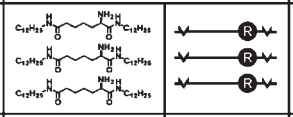	40.5	93.1 / -52.6
2-AupdrnRCs	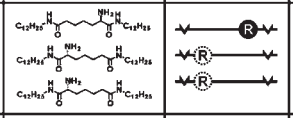	43.4	93.4 / -50.0
3-AupdnRCs	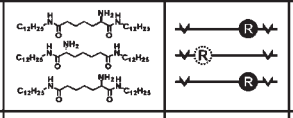	44.0	93.9 / -49.9
4-AdRCs	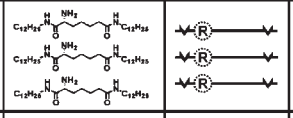	44.4	93.4 / -49.0
5-AupdRCo	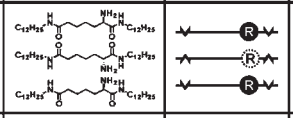	53.9	93.2 / -39.3
6-AupnRCo	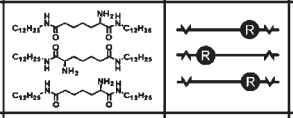	54.8	92.6 / -37.8
7-AdnRCo	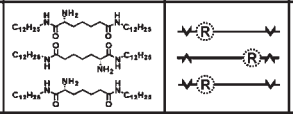	56.7	93.7 / -37.0

[a] Compounds with an odd number of methylene groups force the hydrogen-bonding amide groups to be oriented parallel. (1) All amines up (Aup), in a row (R), and carbonyls in same direction (Cs). (2) Amines randomly up and down (Arupd), not in a row (nR), and carbonyls in same direction (Cs). (3) Amines alternating up and down (Aupd), not in a row (nR), and carbonyls in same direction (Cs). (4) All amines down (Ad), in a row (R), and carbonyls in same direction (Cs). (5) Amines alternating up and down (Aupd), in a row (R), and carbonyls in opposite direction (Co). (6) All amines up (Aup), not in a row (nR), and carbonyls in opposite direction (Co). (7) All amines down (Ad), not in a row (nR), and carbonyls in opposite direction (Co). Amines up/down means that the amine groups are pointing away/towards the substrate surface, respectively.

Table 2. Five Possible Packing Arrangements for an Enantiopure Even Molecule (illustrated for S-ADA6) with Their Total Potential Energy, Valence, and Nonbond Energy Per Mole Molecule[a]

Packing	Model	Total potential Energy (kcal/mol)	Valence Energy / Non-bond Energy
1-AupRCs	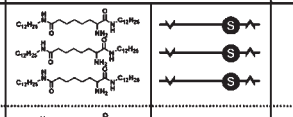	40.0	94.0 / -54.0
2-AuprnRCs	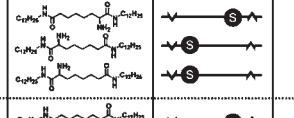	40.6	94.6 / -54.0
3-AupnRCs	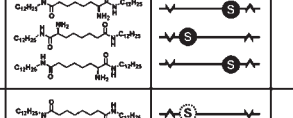	40.7	94.5 / -53.8
4-AdRCs	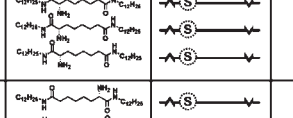	41.9	94.5 / -52.6
5-AupdRCo	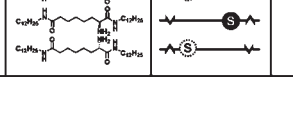	52.4	95.9 / -43.5

[a] Compounds featuring even *n* directs amides (e.g. interacting units) oppositely. (1) All amines up (Aup), in a row (R), and carbonyls in the same direction (Cs). (2) All amines up (Aup), randomly not in a row (rnR), and carbonyls in the same direction (Cs). (3) Amines all up (Aup), alternating not in a row (nR), and carbonyls in the same direction (Cs). (4) All amines down (Ad), not in a row (nR), and carbonyls in the same direction (Cs). (5) Amines alternating up and down (Aupd), in a row (R), and carbonyls in the opposite direction (Co).

From the design considerations above, it is expected that only an enantiomerically pure compound featuring an odd number of methylenes in the spacer will form a patterned monolayer without positional disorder of the amine functionalities.

To further substantiate this hypothesis, molecular mechanics/molecular dynamics (MM/MD) calculations were carried out for enantiopure systems (2 rows of 15−20 molecules) with an odd (e.g., *R*-ADA5) or even (e.g., *S*-ADA6) number of methylenes in the linker connecting both amide groups. All possible packing arrangements were geometry optimized onto a substrate surface made of two frozen graphene layers, and MD simulations were carried out at 298 K for 0.5 ns (see Supporting Information [SI] for more details). The energies discussed were recorded over the last 100 ps of the simulations. These energies were then compared to find the most stable packing. Constraints only apply to the surface. The molecules were completely unconstrained during simulations. As a consequence, the distances that one may measure between those molecules and between molecules and surface reflect the nonbonded interactions.

The *odd* molecule *R*-ADA5 has seven different possible packing arrangements, listed in Table 1. For each packing the total potential energy, the valence, and the nonbond energy were calculated after molecular dynamics. More details can be found in the SI.

The first packing 1-AupRCs has clearly the lowest potential energy. The main difference lies in the nonbond energy. The molecules are able to form very efficient intermolecular hydrogen bonds. The van der Waals energy and the electrostatic interactions also show low (i.e., strongly negative) values since the amine is pointing away from the surface and the distance between the molecules is ideal for favorable interactions. When the amine is directed toward the surface (4-AdRCs), the nonbond energy increases; van der Waals repulsion between the surface and the amine groups results in larger distances between molecules which are detrimental to both hydrogen bonds and electrostatic interactions. When some of the amines are up (alternating (3-AupdnRCs) or random (2-AupdrnRCs)), the van der Waals energy decreases again, and the packing becomes more stable. The last three packing possibilities (5, 6, and 7) in Table 1 all have their carbonyls pointing toward each other. This leads to a significant destabilization and a very unfavorable organization. During the MD run, we observe translations

dx.doi.org/10.1021/ja209018u |*J. Am. Chem. Soc.* 2011, 133, 20942–20950

between molecules, desorption of carbonyls, and flipping on the surface in order to have the carbonyls all pointing in the same direction again.

To find the most stable packing for molecules with an even number of methylene segments between the amide moieties, MD simulations were carried out on different packings of *S*-ADA6. *S*-ADA6 has three different packing possibilities, but for each packing, the molecules can easily rotate 180° around an axis perpendicular to the surface. The position of the amines then changes, but the orientation with respect to the substrate and the orientation of the carbonyls stay the same. These rotations should not affect the total potential energy of the packing, and this was validated for one packing. To find the most stable packing, MD simulations were carried out on five different organizations. The results are shown in Table 2. (For more details, see the SI.)

The first organization (1-AupRCs) with all the amino groups oriented away from the surface and in a row is the most stable one. The difference between the first three organizations (1-AupRCs, 2-AuprnRCs, and 3-AupnRCs) where the amino groups are all pointing up is negligible since it can easily be overcome at room temperature. This means that the position of the amine in a row, alternating or random, does not influence the energy as long as the amines have the same orientation with respect to the substrate. These three organizations have the lowest energy. When all the free amines are pointing toward the substrate (4-AdRCs), the backbone of the molecules has to tilt slightly, leading to less favorable nonbond interactions, mostly van der Waals interactions. When the amines point up and down (5-AudRCo), the carbonyls are directed toward each other. As seen for the *R*-ADA5, this kind of packing costs a lot of energy; in particular, hydrogen bonds and favorable electrostatic interactions will be lost. Overall, the most stable organization is the one with all the amines pointing away from the surface. Since there is no real preference in the position of these amines, the most disordered packing, 2-AuprnRCs, is probably the most favored one, based upon entropy considerations.

Even more possible packing modes are expected when monolayers are formed from a racemate. In general, deposition from a racemate[60−63] can lead to the formation of a racemic conglomerate consisting of enantiomerically pure domains, a racemic compound containing both enantiomers in its unit cell, or a solid solution in which the enantiomers are randomly mixed in the monolayer.[64,65] In contrast to the situation for regular 3D crystallization, the majority of the racemates investigated so far at the liquid/solid interface form monolayers that are racemic conglomerates.[66] In 3D, inversion centers create the most dense packing which implies racemic compound formation, while in 2D, 2-fold rotations are responsible for the densest packing since inversion centers are not compatible with a plane, meaning that generally in 2D enantiomerically pure domains are favored. For racemates of ADA molecules with parallel oriented amides, each of these possibilities is equally likely, though, if one considers similar qualitative stability criteria as for monolayers consisting of enantiopure compounds. However, racemates of ADA molecules with antiparallel oriented amides are expected to self-assemble into racemic conglomerates.

Synthesis. The design of the compounds is based on α-amino diamides, which can be derived from commercially available α-amino diacids via the well-established synthesis of amides (Scheme 1). *N*-Boc-α-amino diacids were reacted with 2 equiv of dodecyl amine to give the crude bis-amides **2a**−**g**. Extensive purification followed by removal of the boc-protecting group in acidic conditions gave the bis-amide ammonium salts **3a**−**g**, which without further purification were treated with base to give the final products **4a**−**g**. Compound **4h** was prepared starting from α-(Fmoc)-amino diacid which was also coupled with 2 equiv of dodecyl amine, followed by removal of the Fmoc protecting group to give directly **4h**. All compounds were characterized by ^{1}H NMR, ^{13}C NMR, MS, and elemental analysis (final products only). Characterization as well as detailed synthetic procedures can be found in the SI.

STM. To test the hypothesis on interfacial arrangement of functional bisamides, the self-assembly of these compounds was studied with STM. Solutions of the ADA-molecules were prepared in 1-phenyloctane (2.10−4 mol/L) by gentle heating (60 °C). Then a droplet of the solution at room temperature was applied on the basal plane of highly oriented pyrolytic graphite (HOPG) (1 × 1 cm^2) at room temperature. A sketch of the substrate with its symmetry axes is shown in the SI. Typically, 30 min after deposition of a drop of the solution on the basal plane of graphite, the outcome of the self-assembly process was probed by STM at the 1-phenyloctane/HOPG interface.

While MM/MD have been carried out on the odd *R*-ADA5 and the even *S*-ADA6, STM studies of monolayer formation have been carried out for a broader spectrum of compounds, ranging from small (ADA3) to long (ADA6).

For the odd enantiopure molecules *R*-ADA3 and *S*-ADA3, the molecules are stacked and form a closely packed lamellar structure (Figure 3). Each molecule consists of two darker parts and a brighter part. The alkyl chains have a lower tunneling efficiency and appear quite dark in the STM image, while the amine groups have a higher tunneling efficiency and appear fairly bright. The STM contrast provides no direct information on the orientation of the amine groups. On the basis of the simulations, though, we assume that the amine groups are directed away from the surface. This also holds for the other molecules. Both *R*- and *S*-ADA3 have a lamella width of 4.0 ± 0.1 nm, and the distance between two successive molecules in a lamella is 0.48 ± 0.05 nm. The difference in packing for these two molecules lies in the orientation of the lamella direction with respect to the normal of the main symmetry axes of the underlying graphite substrate ⟨1−100⟩, shown in Figure 3. This angle is +2 ± 1° for *R*-ADA3 and −3 ± 1° for *S*-ADA3 (SI), which means that the absolute chirality of the molecules is expressed in the monolayer orientation with respect to graphite. The alkyl chains are lying parallel with the main symmetry axes of graphite ⟨11−20⟩. The amine groups seem to be aligned in a row. Especially the high-resolution image of *S*-ADA3 shows that the bright dots are in a straight line. To quantify the ordering of the amines, a correlation factor was calculated. The number of hetero pairs (adjacent amines on opposite sites) was divided by the number of homo pairs (adjacent amines on the same side). In this case a correlation factor of 0.09 was found, which substantiates the conclusion that the amines are ordered in a row. Assuming that this correlation factor reflects the equilibrium constant K = [hetero pair]/[homo pair], the standard free energy change $\Delta G^\circ_{\text{ho-he}}$ for a hypothetical process where a hetero pair is converted into a homo pair measures −1.42 kcal/mol. Overall, the pattern can be described as 1-AupRCs, in line with MM/MD predictions.

As a comparison, the self-assembly of the even enantiopure molecules *R*-ADA4 and *S*-ADA4 was also studied. Figure 4 shows that these molecules stack into closely packed lamella too. The lamella width is 4.1 ± 0.1 nm, the distance between two

Scheme 1. Synthesis of ADA Molecules[a]

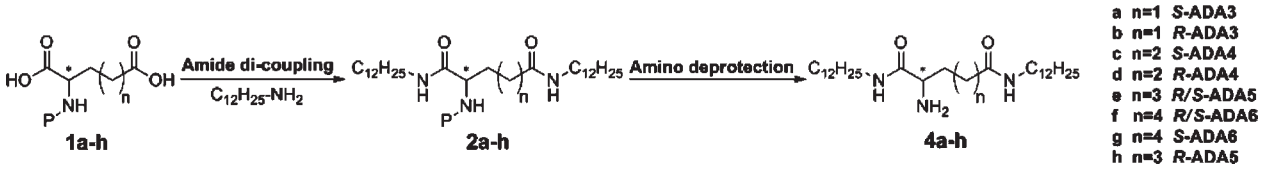

[a] P represents the protecting group. On the right side the number of methylene groups *n* and the absolute configuration of the enantiocenter are defined for any compound.

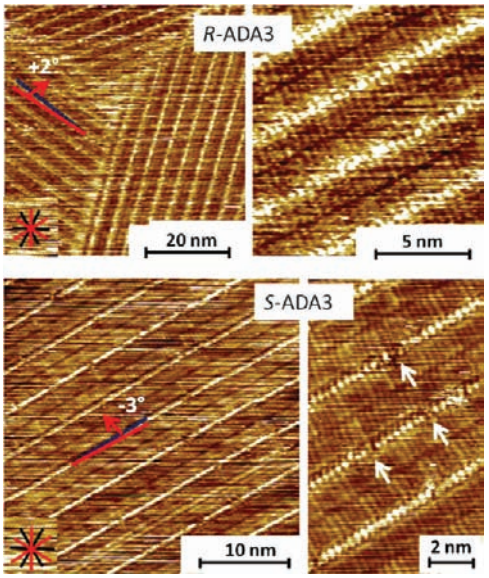

Figure 3. STM-images of *R*-ADA3 (first row) and *S*-ADA3 (second row). I_{set} = 79 pA, V_{set} = −1040 mV. (Inset) Underlying graphite substrate with its main symmetry axes ⟨11−20⟩ in black and the normals of the main symmetry axes ⟨1−100⟩ in red. The angle between the lamella direction (blue) and a normal of the main symmetry axes (red) is indicated. The white arrows show missing amines.

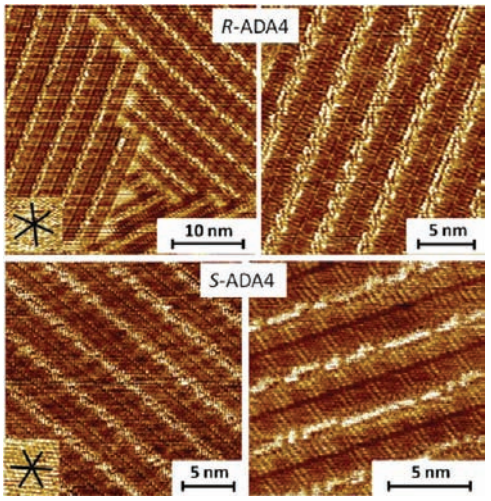

Figure 4. STM images of *R*-ADA4 (first row) and *S*-ADA4 (second row). I_{set} = 24 pA, V_{set} = −860 mV. (Inset) Underlying graphite substrate with its main symmetry axes ⟨11−20⟩.

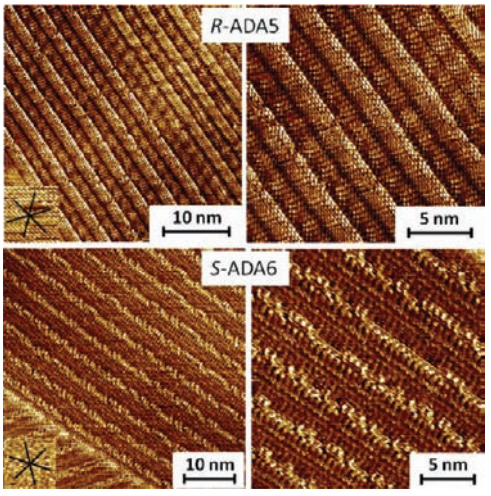

Figure 5. STM-images of *R*-ADA5 (first row) and *S*-ADA6 (second row). I_{set} = 86 pA, V_{set} = −1040 mV. (Inset) Underlying graphite substrate with its main symmetry axes ⟨11−20⟩.

neighboring molecules is 0.48 ± 0.05 nm, and the alkyl chains lie parallel with the main symmetry axes of graphite ⟨11−20⟩. The chirality of *R*- and *S*-ADA4 is again expressed in the orientation of the lamella direction with respect to the normal of the main symmetry axes of graphite ⟨1−100⟩. For *R*-ADA4, this angle measures −4 ± 1°; for *S*-ADA4 it is +3 ± 1°. For few domains the even molecules *S*- and *R*-ADA4 also show a second polymorph. More details can be found in the SI. In contrast to the odd molecules *R*- and *S*-ADA3, the amines do not appear as a single bright line, indicating they are randomly oriented. Within a row of stacked molecules, two bright but discontinuous lines can be seen, which are attributed to the location of the amine groups. This suggests that the molecules can rotate 180° around an axis perpendicular to the surface, due to the quasi-C_2 symmetry of the amide moieties. In the high-resolution image of *S*-ADA4, the hopping from 'left' amines to 'right' amines is clearly visualized. In the case of enantiopure even molecules a correlation factor of 0.86 was obtained ($\Delta G^{\circ}_{ho\text{-}he}$ = 0.089 kcal/mol), which confirms the random orientation. The pattern can be described as 2-AuprnRCs, in line with the MM/MD predictions

When the spacer becomes longer, it should be easier to visualize if the amines are in a line or randomly organized. To evaluate if the self-assembly does not change by varying the length of the spacer and to confirm the observed odd/even effect, the self-assembly of *R*-ADA5 and *S*-ADA6 was studied and compared with the outcome of the MM/MD simulations (Tables 1 and 2). *R*-ADA5 assembles into lamella with a width of 4.3 ± 0.1 nm (Figure 5), which is naturally larger than that of the shorter analogues. The distance between two neighboring molecules is 0.48 ± 0.02 nm, and the alkyl chains lie parallel with the main symmetry axes of graphite ⟨11−20⟩. The angle between

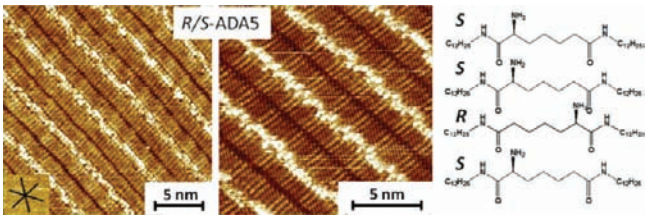

Figure 6. STM-images of *R*-/*S*-ADA5. I_{set} = 137 pA, V_{set} = −680 mV. (Inset) Underlying graphite substrate with its main symmetry axes ⟨11−20⟩. The right scheme shows how *R* and *S* enantiomers can be mixed within the same lamella with no significant energy loss.

the direction of the lamella and the normal of the underlying symmetry axes of graphite ⟨1−100⟩ is +4 ± 1°. The free amines are clearly in a straight line These results confirm that enantiopure odd ADA molecules give rise to closely packed lamella with its free amines ordered in a row. Therefore, 1-AupRCs is the most stable packing, and this is in agreement with the predictions. The calculated unit cell parameters, shown in the SI, are also consistent with the measured unit cell parameters.

In every STM-image, though, there are some bright dots missing in the row of amines. This is probably due to the fact that a molecule has flipped and rotated so that the carbonyls are still directed in the same direction, but the amine is now pointing toward the surface and is not lying in the row anymore. In the packing possibilities (Table 1), the random packing 2-AupdrnRCs is the closest in energy in comparison with the most stable packing. Therefore, this organization is very probable as a defect. The other possible defects are unlikely to occur because of their high energy penalty. This was verified with a separate set of calculations which determined the energy cost of different possible defects and is shown in the SI.

The even *S*-ADA6 molecules self-assemble into lamella with a width of 4.3 ± 0.1 nm (Figure 5). The distance between two neighboring molecules is 0.49 ± 0.02 nm and the alkyl chains lie parallel with the main symmetry axes of graphite ⟨11−20⟩. The angle between the direction of the lamella and the normal of the underlying symmetry axes of graphite ⟨1−100⟩ is −6 ± 1°. Also for even *S*-ADA6 molecules a second polymorph is found. Because only a few domains with this packing have been observed, this polymorph is described in the SI. In contrast to the odd molecules and similar to the even *R*- and *S*-ADA4 molecules, the amines appear randomly ordered. This organization is in line with the predictions in which the amines are packed randomly in a row, and with the experimental data on the ADA4.

The calculated unit cell parameters, shown in the SI, are also consistent with the measured unit cell parameters.

In conclusion, using odd ADA molecules, the amine groups can be forced to line up, having most probably their amino groups pointing toward the supernatant solution. For even ADA molecules, this is not possible. An odd/even effect, in combination with the use of enantiomers, can be combined to direct the position of functional groups in a 2D supramolecular lattice.

Self-assembly of enantiopure ADA compounds is absolutely necessary to force the amino functionality to be in line in a supramolecular tape. This is proven by experiments where a racemate rather than an enantiopure compound was allowed to self-assemble at the liquid/solid interface. To simplify the analysis of the STM data, only racemates of the longest odd and even ADA molecules were investigated.

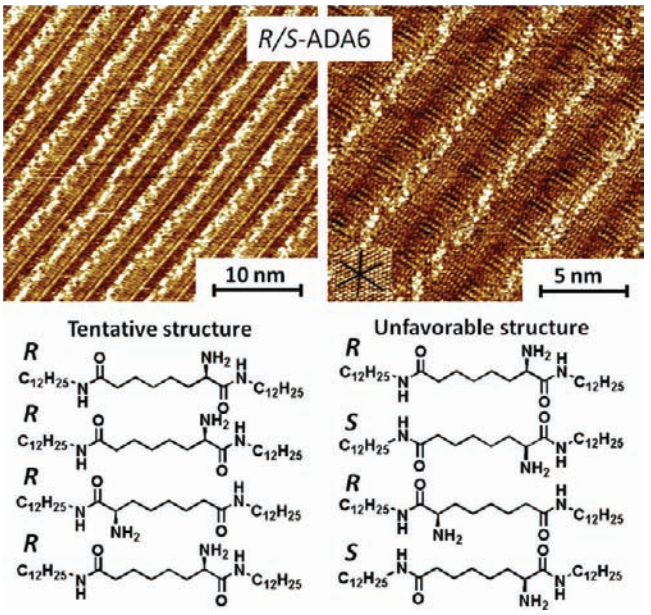

Figure 7. Molecular structure and STM-images of *R*/*S*-ADA6. I_{set} = 100 pA, V_{set} = −760 mV. (Inset) Underlying graphite substrate with its main symmetry axes. (Bottom left) Tentative arrangement of molecules in enantiopure lamellae featuring disordered amines. (Bottom right) Demonstrates that *R*- and *S*-enantiomers cannot be mixed within the same lamella without significant energy loss.

R-/*S*-ADA5, representative for the odd molecules, self-assembles into closely packed lamella with a width of 4.2 ± 0.1 nm. The distance between two neighboring molecules is 0.48 ± 0.01 nm, and the alkyl chains lie parallel with the main symmetry axes of graphite ⟨11−20⟩. The angle between the direction of the lamella and the normal of the symmetry axes ⟨1−100⟩ of graphite is now smaller and varies between −2° and +2° ± 1°. Figure 6 shows a high-resolution STM-image of the monolayer formed from the racemate. In contrast with the pure odd enantiomer, the amines are not lying in a row. They are randomly organized (correlation factor of 1.08). Assuming that the amine groups are directed away from the surface, modeling predicts that such a situation can only occur if both enantiomers coadsorb in the same hydrogen bonded row, since the carbonyls would otherwise be directed toward each other which is very unlikely due to significant destabilization. Since this mixing is random, a solid solution is formed.[67] MD/MM were carried out (SI) and showed that both a racemic compound and a racemic conglomerate could be formed also, but since there is no significant difference in stability, the most disordered packing is normally favored on the basis of entropy considerations, which is in agreement with the formation of a solid solution, and the experimental data.

R-/*S*-ADA6, the representative of the even molecules, also self-assembles into closely packed lamella with a width of 4.3 ± 0.1 nm (Figure 7). The distance between two neighboring molecules is 0.48 ± 0.01 nm and the alkyl chains lie parallel with the main symmetry axes of graphite ⟨11−20⟩. The angle between the lamella direction and the normal of the symmetry axes ⟨1−100⟩ of graphite varies between −2° and +2° ± 1°.

The STM images show that the amines are randomly ordered (correlation factor of 1.03). However, note that rows of enantiopure molecules are themselves structurally disordered which complicates the analysis of the STM data. However, most likely,

the *R*- and *S*-enantiomers are not mixed in a lamella because mixing *R*-ADA and *S*-ADA6 with all the amines standing up would force carbonyl groups to be oriented toward each other (Figure 7 bottom right) and as shown by the MM/MD simulations this is energetically very unfavorable. We can conclude that at the level of the lamellae a racemic conglomerate is formed, since each lamella is enantiomerically pure (Figure 7 bottom left). At larger length scales, different domains (+2 and −2 with respect to graphite) can be found. Although these angles are quite small, they are consistent with the previous enantiopure experiments. This suggests that lamellae of *R* and *S* molecules are separated into different domains and a racemic conglomerate is formed. With more certainty, we can state that at the level of the lamellae, a racemic conglomerate is formed. Similar to the enantiopure even enantiomers, the racemate also gives rise to a second polymorph, a racemic compound (see SI). Molecular dynamics confirmed that both a racemic conglomerate and a racemic compound, but with enantiopure lamellae, are probable (see SI).

Monolayers formed from a racemate of odd or even ADA molecules always contain randomly organized amines which are most likely oriented away from the surface. For odd molecules, a solid solution is formed, while for even molecules, the formation of a racemic conglomerate was deduced. The differences in the patterns formed by racemates of compounds with different alkyl chain parity can be explained by the dominant role of hydrogen-bonding. Hydrogen bonding between amide groups determines the possible relative orientations of interacting molecules. The position of the amino group along the alkyl spacer is not a determining factor. As a result, for ADA molecules with odd parity, enantiomers can be part of the same row. From an enthalpy point of view, there is no preference for the formation of a solid solution, racemic compound, or racemic conglomerate. On the basis of entropy considerations though, a solid solution is favored. For molecules with an even spacer, the enantiomers are forced to assemble in separate rows.

CONCLUSIONS

This study shows that it is possible to control the spatial deposition of functional moieties at the graphite−liquid interface with subnanometer precision, by employing physisorbed monolayers as a topological scaffold. As a model system, linear bis-amides as a supramolecular scaffold with pendant amine functions have been designed and synthesized by employing hydrogen bonding as the dominant intermolecular interaction and taking into account (i) molecular symmetry governed by odd−even effects and (ii) chirality selection - to control their ordering on surfaces. The predictions from these qualitative design considerations were confirmed by quantitative MM/MD simulations, and STM studies revealed that the linear bis-amides with pendant amines indeed form physisorbed monolayers at the graphite/phenyl octane interface. The monolayers have a regular, lamellar structure but with various degree of order within the lamella, depending on the molecular symmetry and enantiomeric composition of the compound.

The following key guidelines proved to be successful to control the positioning of functional groups, i.e. amino groups, on a surface, obviously under conditions wherein self-assembly into monolayers takes place.

(i) The most bulky group on a stereogenic center on an alkyl chain tends to be directed away from the graphite substrate. This intuitive guideline is very useful, especially considering systems with multiple groups or chiral centers. Note that some exceptions have been reported though.[68]

(ii) Directional intermolecular interactions (e.g., hydrogen bonding), in combination with molecular symmetry, facilitate the prediction of the self-assembly process. A particular useful and reliable way to influence molecular symmetry is based on alkyl spacer parity.

Following these guidelines, it was predicted and experimentally shown that the only successful approach to align amine groups in a row, based on the ADA motif, is via enantiopure molecules with an odd number of methylene groups in the alkyl spacer connecting both amide groups. Adsorption of enantiopure molecules with an even number of methylene groups or from a racemate of both odd and even ADAs gives rise to randomly ordered amines.

In addition to the success in positioning functional groups with high spatial control, this study also gave insight into factors which govern the formation of a solid solution, racemic compound, or racemic conglomerate. This is relevant as most of the systems investigated so far at the liquid/solid interface gave rise to racemic conglomerate formation. Under the conditions (i) that the self-assembly system is characterized by strong intrarow directional noncovalent interactions dictating the possible orientations of adjacent molecules and (ii) that the chiral center determines which side of the molecule faces the surface, the alkyl chain parity will determine if a racemic conglomerate or solid solution is formed, at least at the level of the individual lamella.

The ease of formation, the stability of these monolayers, and the accessibility of the amine groups, directed away from the surface, opens the way to use these monolayers as templates for synthesis at the liquid/solid interface.

ASSOCIATED CONTENT

Supporting Information. S1 - Detailed information about the synthesis of the different compounds. S2 - Experimental details on molecular mechanics and molecular dynamics. S3 - Energies of different packing of *R*-ADA5. S4 - Unit cell parameters for *R*-ADA5 AupRCs. S5 - Energies of different packing of *S*-ADA6. S6 - Unit cell parameters for *S*-ADA6 AuprnRCs. S7 - Experimental details on STM measurements. S8 - The graphite surface and its symmetry axes. S9 - Angle of lamella direction with respect to graphite ⟨1−100⟩ axes. S10 - STM measurements and analysis of second polymorph even molecules. S11 - Energy cost of a defect. S12 - MM/MD calculations on various packings composed of an equimolar mixture of both enantiomers of ADA5. S13 - MM/MD calculations on various packings composed of an equimolar mixture of both enantiomers of ADA6. S14 - Second polymorph of racemic mixture of *R*-/*S*-ADA6. This material is available free of charge via the Internet at http://pubs.acs.org.

AUTHOR INFORMATION

Corresponding Author
Steven.DeFeyter@chem.kuleuven.be; J.H.vanEsch@tudelt.nl

ACKNOWLEDGMENT

The research leading to these results has received funding from the European Community's Seventh Framework Program under Grant Agreement NMP4-SL-2008-214340, project RESOLVE. Furthermore, this work is supported by the Fund of Scientific Research - Flanders (FWO), K.U.Leuven (GOA),

the Belgian Federal Science Policy Office through IAP-6/27, and the Institute for the Promotion of Innovation by Science and Technology in Flanders (IWT). Research in Mons is also supported by the OPTI2MAT Excellence program of Région Wallonne and by FNRS-FRFC. C.G. is supported by an ERA Chemistry/NWO grant and J.v.E. by a NWO VICI grant. The authors thank Dr. K. Djanashvili for advice with NMR measurements.

REFERENCES

(1) Lewis, P. A.; Donhauser, Z. J.; Mantooth, B. A.; Smith, R. K.; Bumm, L. A.; Kelly, K. F.; Weiss, P. S. *Nanotechnology* **2001**, *12*, 231–237.
(2) Menard, E.; Meitl, M. A.; Sun, Y. G.; Park, J. U.; Shir, D. J. L.; Nam, Y. S.; Jeon, S.; Rogers, J. A. *Chem. Rev.* **2007**, *107*, 1117–1160.
(3) Mendes, P. M.; Yeung, C. L.; Preece, J. A. *Nanoscale Res. Lett.* **2007**, *2*, 373–384.
(4) Cavallini, M.; Albonetti, C.; Biscarini, F. *Adv. Mater.* **2009**, *21*, 1043–1053.
(5) Joe, M.; Kim, J. H.; Choi, C.; Kahng, B.; Kim, J. S. *J. Phys.: Condens. Matt.* **2009**, *21*, 224011.
(6) Simeone, F. C.; Albonetti, C.; Cavallini, M. *J. Phys. Chem. C* **2009**, *113*, 18987–18994.
(7) Hoeppener, S.; Chi, L. F.; Fuchs, H. *Nano Lett.* **2002**, *2*, 459–463.
(8) Bonifazi, D.; Kiebele, A.; Stohr, M.; Cheng, F. Y.; Jung, T.; Diederich, F.; Spillmann, H. *Adv. Funct. Mat.* **2007**, *17*, 1051–1062.
(9) Mao, G.; Dong, W.; Kurth, D. G.; Möhwald, H. *Nano Lett.* **2004**, *4*, 249–252.
(10) Love, J. C.; Estroff, L. A.; Kriebel, J. K.; Nuzzo, R. G.; Whitesides, G. M. *Chem. Rev.* **2005**, *105*, 1103–1169.
(11) Vericat, C.; Vela, M. E.; Salvarezza, R. C. *Phys. Chem. Chem. Phys.* **2005**, *7*, 3258–3268.
(12) Haussling, L.; Michel, B.; Ringsdorf, H.; Rohrer, H. *Angew. Chem., Int. Ed.* **1991**, *30*, 569–572.
(13) Spinke, J.; Liley, M.; Guder, H. J.; Angermaier, L.; Knoll, W. *Langmuir* **1993**, *9*, 1821–1825.
(14) Ferretti, S.; Paynter, S.; Russell, D. A.; Sapsford, K. E.; Richardson, D. J. *TrAC, Trends Anal. Chem.* **2000**, *19*, 530–540.
(15) Nelson, K. E.; Gamble, L.; Jung, L. S.; Boeckl, M. S.; Naeemi, E.; Golledge, S. L.; Sasaki, T.; Castner, D. G.; Campbell, C. T.; Stayton, P. S. *Langmuir* **2001**, *17*, 2807–2816.
(16) Berner, S.; Biela, S.; Ledung, G.; Gogoll, A.; Backvall, J. E.; Puglia, C.; Oscarsson, S. *J. Catal.* **2006**, *244*, 86–91.
(17) Hara, K.; Akiyama, R.; Takakusagi, S.; Uosaki, K.; Yoshino, T.; Kagi, H.; Sawamura, M. *Angew. Chem., Int. Ed.* **2008**, *47*, 5627–5630.
(18) Marshall, S. T.; O'Brien, M.; Oetter, B.; Corpuz, A.; Richards, R. M.; Schwartz, D. K.; Medlin, J. W. *Nat. Mater.* **2010**, *9*, 853–858.
(19) Paluti, C. C.; Gawalt, E. S. *J. Catal.* **2010**, *275*, 149–157.
(20) Mrksich, M.; Whitesides, G. M. *Trends Biotechnol.* **1995**, *13*, 228–235.
(21) Mendes, R. K.; Carvalhal, R. F.; Kubota, L. T. *Electroanal. Chem.* **2008**, *612*, 164–172.
(22) Yang, G. H.; Qian, Y. L.; Engtrakul, C.; Sita, L. R.; Liu, G. Y. *J. Phys. Chem. B.* **2000**, *104*, 9059–9062.
(23) Huskens, J.; Deij, M. A.; Reinhoudt, D. N. *Angew. Chem., Int. Ed.* **2002**, *41*, 4467–4471.
(24) Pace, G.; Petitjean, A.; Lalloz-Vogel, M. N.; Harrowfield, J.; Lehn, J. M.; Samori, P. *Angew. Chem., Int. Ed.* **2008**, *47*, 2484–2488.
(25) Ciesielski, A.; Stefankiewicz, A. R.; Hanke, F.; Persson, M.; Lehn, J. M.; Samori, P. *Small* **2011**, *7*, 342–350.
(26) Wilbur, J. L.; Kumar, A.; Kim, E.; Whitesides, G. M. *Adv. Mater.* **1994**, *6*, 600–604.
(27) Jiang, L.; Wang, W. C.; Fuchs, H.; Chi, L. F. *Small* **2009**, *5*, 2819–2822.
(28) Kramer, S.; Fuierer, R. R.; Gorman, C. B. *Chem. Rev.* **2003**, *103*, 4367–4418.
(29) Elemans, J. A. A. W.; Lensen, M. C.; Gerritsen, J. W.; van Kempen, H.; Speller, S.; Nolte, R. J. M.; Rowan, A. E. *Adv. Mater.* **2003**, *15*, 2070–2073.
(30) Samori, P.; Engelkamp, H.; de Witte, P.; Rowan, A. E.; Nolte, R. J. M.; Rabe, J. P. *Angew. Chem., Int. Ed.* **2001**, *40*, 2348–2350.
(31) Wan, L.-J. *Acc. Chem. Res.* **2006**, *39*, 334–342.
(32) Mu, Z.; Shu, L.; Fuchs, H.; Mayor, M.; Chi, L. *J. Am. Chem. Soc.* **2008**, *130*, 10840–10841.
(33) Clair, S.; Abel, M.; Porte, L. *Angew. Chem., Int. Ed.* **2010**, *49*, 8237–8239.
(34) Rabe, J. P.; Buchholz, S. *Science* **1991**, *253*, 424–427.
(35) Rabe, J. P.; Buchholz, S. *Phys. Rev. Lett.* **1991**, *66*, 2096–2099.
(36) Buchholz, S.; Rabe, J. P. *Angew. Chem., Int. Ed.* **1992**, *31*, 189–191.
(37) Cyr, D. M.; Venkataraman, B.; Flynn, G. W.; Black, A.; Whitesides, G. M. *J. Phys. Chem.* **1996**, *100*, 13747–13759.
(38) De Feyter, S.; Grim, P. C. M.; van Esch, J.; Kellogg, R. M.; Feringa, B. L.; De Schryver, F. C. *J. Phys. Chem. B* **1998**, *102*, 8981–8987.
(39) Cyr, D. M.; Venkataraman, B.; Flynn, G. W. *Chem. Mater.* **1996**, *8*, 1600–1615.
(40) Giancarlo, L. C.; Flynn, G. W. *Annu. Rev. Phys. Chem.* **1998**, *49*, 297–336.
(41) Giancarlo, L. C.; Flynn, G. W. *Acc. Chem. Res.* **2000**, *33*, 491–501.
(42) De Feyter, S.; De Schryver, F. C. *Chem. Soc. Rev.* **2003**, *32*, 139–150.
(43) De Feyter, S.; Larsson, M.; Schuurmans, N.; Verkuijl, B.; Zoriniants, G.; Gesquiere, A.; Abdel-Mottaleb, M. M.; van Esch, J.; Feringa, B. L.; van Stam, J.; De Schryver, F. C. *Chem.—Eur. J.* **2003**, *9*, 1198–1206.
(44) Kudernac, T.; Lei, S. B.; Elemans, J.; De Feyter, S. *Chem. Soc. Rev.* **2009**, *38*, 402–421.
(45) Elemans, J.; Lei, S. B.; De Feyter, S. *Angew. Chem., Int. Ed.* **2009**, *48*, 7298–7332.
(46) Gutzler, R.; Lappe, S.; Mahata, K.; Schmittel, M.; Heckl, W. M.; Lackinger, M. *Chem. Commun.* **2009**, 680–682.
(47) Llanes-Pallas, A.; Palma, C. A.; Piot, L.; Belbakra, A.; Listorti, A.; Prato, M.; Samori, P.; Armaroli, N.; Bonifazi, D. *J. Am. Chem. Soc.* **2009**, *131*, 509–520.
(48) Matena, M.; Llanes-Pallas, A.; Enache, M.; Jung, T.; Wouters, J.; Champagne, B.; Stohr, M.; Bonifazi, D. *Chem. Commun.* **2009**, 3525–3527.
(49) Popoff, A.; Fichou, D. *J. Mol. Struct.* **2009**, *936*, 156–161.
(50) Grill, L.; Dyer, M.; Lafferentz, L.; Persson, M.; Peters, M. V.; Hecht, S. *Nat. Nanotechnol.* **2007**, *2*, 687–691.
(51) Grim, P. C. M.; De Feyter, S.; Gesquière, A.; Vanoppen, P.; Rucker, M.; Valiyaveettil, S.; Moessner, G.; Mullen, K.; De Schryver, F. C. *Angew. Chem., Int. Ed.* **1997**, *36*, 2601–2603.
(52) Schmitz, C. H.; Ikonomov, J.; Sokolowski, M. *J. Phys. Chem. C* **2009**, *113*, 11984–11987.
(53) Weigelt, S.; Busse, C.; Bombis, C.; Knudsen, M. M.; Gothelf, K. V.; Laegsgaard, E.; Besenbacher, F.; Linderoth, T. R. *Angew. Chem., Int. Ed.* **2008**, *37*, 4406–4410.
(54) Zwaneveld, N. A. A.; Pawlak, R.; Abel, M.; Catalin, D.; Gigmes, D.; Bertin, D.; Porte, L. *J. Am. Chem. Soc.* **2008**, *130*, 6678–6679.
(55) Florio, G. M.; Werblowskyf, T. L.; Ilan, B.; Muller, T.; Berne, B. J.; Flynn, G. W. *J. Phys. Chem. C* **2008**, *112*, 18067–18075.
(56) Wei, Y. H.; Kannappan, K.; Flynn, G. W.; Zimmt, M. B. *J. Am. Chem. Soc.* **2004**, *126*, 5318–5322.
(57) Nath, K. S.; Ivasenko, O.; Macleod, J. M.; Miwa, J. A.; Wuest, J. D.; Nanci, A.; Perepichka, D. F.; Rosei, F. *J. Phys. Chem. C* **2007**, *111*, 16996–17007.
(58) Mali, K. S.; Lava, K.; Binnemans, K.; De Feyter, S. *Chem.—Eur. J.* **2010**, *16*, 14447–14458.
(59) Tao, F.; Bernasek, S. L. *Chem. Rev.* **2007**, *107*, 1408–1453.
(60) Romer, S.; Behzadi, B.; Fasel, R.; Ernst, K. H. *Chem.—Eur. J.* **2005**, *11*, 4149–4154.
(61) Ilan, B.; Berne, B. J.; Flynn, G. W. *J. Phys. Chem. C* **2007**, *49*, 18243–18250.

(62) Mamdouh, W.; Uji-i, H.; Gesquiere, A.; De Feyter, S.; Amabilino, D. B.; Abdel-Mottaleb, M. M. S.; Veciana, J.; De Schryver, F. C. *Langmuir* **2004**, *20*, 9628–9635.
(63) Forster, M; Dyer, M. S.; Barrett, S. D.; Persson, M.; Raval, R. *J. Phys. Chem. C* **2011**, *115*, 1180–1185.
(64) Perez-Garcia, L.; Amabilino, D. B. *Chem. Soc. Rev.* **2002**, *31*, 342–356.
(65) Elemans, J. A. A. W.; De Cat, I.; Xu, H.; De Feyter, S. *Chem. Soc. Rev.* **2009**, *38*, 722–736.
(66) Plass, K. E.; Grzesiak, A. L.; Matzger, A. J. *Acc. Chem. Res.* **2007**, *40*, 287–293.
(67) Bieger, D.; Kreher, D.; Mathevet, F.; Attias, A. J.; Schull, G.; Huard, A.; Douillard, L.; Fiorini-Debuischert, C.; Charra, F. *Angew. Chem., Int. Ed.* **2007**, *46*, 7404–7407.
(68) Iavicoli, P.; Xu, H.; Feldborg, L. N.; Linares, M.; Paradinas, M.; Stafstrom, S.; Ocal, C.; Nieto-Ortega, B. L.; Casado, J.; Navarrete, J. T. L.; Lazzaroni, R.; De Feyter, S.; Amabilino, D. B. *J. Am. Chem. Soc.* **2010**, *132*, 9350–9362.